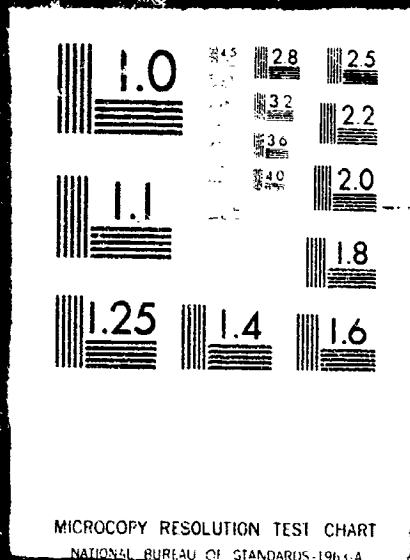


1 OF 1

N72 16334 UNCLAS



**NASA TECHNICAL  
MEMORANDUM**

NASA TM X-68002

NASA TM X-68002

**ANALYSIS OF AN ARCHED OUTER-RACE BALL  
BEARING CONSIDERING CENTRIFUGAL FORCES**

by Bernard J. Hamrock and William J. Anderson  
Lewis Research Center  
Cleveland, Ohio

TECHNICAL PAPER proposed for presentation at  
Lubrication Conference cosponsored by the  
American Society of Mechanical Engineers and  
the American Society of Lubrication Engineers  
New York, New York, October 9-12, 1972



802  
(ACCESSION NUMBER)  
(NASA-TM-X-68002) ANALYSIS OF AN ARCHED  
OUTER-FACE BALL BEARING CONSIDERING  
CENTRIFUGAL FORCES S. J. HAMROCK, et al  
(NASA) PILLLEGAL DATE? 23 D CSCL 131

N72-16334

Unclass  
14251

33/15

ANALYSIS OF AN ARCHED OUTER-RACE BALL BEARING  
CONSIDERING CENTRIFUGAL FORCES

by Bernard J. Hanrock and William J. Anderson

Lewis Research Center  
Cleveland, Ohio

ABSTRACT

12-5795

A thrust load analysis of an arched outer race ball bearing which considers centrifugal forces but which neglects gyroscopics, elasto-hydrodynamics, and thermal effects was performed. A Newton-Raphson method of iteration was used in evaluating the radial and axial projection of the distance between the ball center and the outer raceway groove curvature center ( $V$  and  $W$ ). Fatigue life evaluations were made. The similar analysis of a conventional bearing can be directly obtained from the arched bearing analysis by simply letting the amount of arching be zero ( $g = 0$ ) and not considering equations related to the unladed half of the outer race.

The analysis was applied to a 150-mm angular contact ball bearing. Results for life, contact loads, and angles are shown for a conventional bearing ( $g = 0$ ) and two arched bearings ( $g = 0.127$  mm (0.005 in.), and 0.254 mm (0.010 in.)). The results indicate that an arched bearing is highly desirable for high speed applications. In particular, for a DN value of 3 million (20 000 rpm) and an applied axial load of 4448 N (1000 lb), an arched bearing shows an improvement in life of 366 percent over that of a conventional bearing. At 4.2 million DN (28 000 rpm) the corresponding improvement is 340 percent. It was also found for low speeds, the arched bearing does not offer the advantages that it does for high speed applications.

INTRODUCTION

Aircraft gas turbine engine rotor bearings currently operate in the speed range from 1.5 to 2 million DN (bearing bore in mm times shaft

speed in rpm). It is estimated that engine designs of the next decade will require bearings to operate at DN values of 3 million or more (ref. 1). In this DN range, analyses (refs. 2 and 3) predict a prohibitive reduction in bearing fatigue life due to the high centrifugal forces developed between the rolling elements and outer race.

Several approaches to the high speed bearing problem have been suggested and are being developed. One approach is to reduce ball mass through the use of thin wall spherically hollow balls (ref. 4) or drilled balls (refs. 5, 6, and 7). Theory indicates that significant improvements in bearing fatigue life can be obtained at DN values of 3 million and above with a 50 percent or greater weight removal from the balls. Flexure failures have occurred with both hollow and drilled balls after short running times, however, so both of these concepts must still be considered highly experimental.

Hybrid bearings consisting of a combination ball and fluid film bearing constitute a second approach. The parallel hybrid bearing (ref. 8), in which the fluid film bearing and ball bearing share the system load with both operating at full speed, can be used to improve high speed ball bearing life. However, the effectiveness of the parallel hybrid bearing diminishes at high speeds because it does not attenuate centrifugal effects in the ball bearing. The series hybrid bearing (refs. 9 and 10), in which a fluid film bearing and ball bearing both carry full system load while each operates at part speed, is theoretically the most effective approach to extending high speed ball bearing life. This concept, too, is still quite experimental. Mechanical complexity is a problem, and effects on shaft stiffness and rotor dynamics must be evaluated.

Initial experiments with an arched outer-race ball bearing (ref. 11) indicated that this design operated with lower torque than a conventional angular contact bearing. The experiments of reference 11 were conducted at DN values up to about 1 million. In light of the successful experiments of reference 11, the arched outer-race ball bearing seemed to be a promising high speed bearing concept because of its ability to share the centrifugal loading at two outer-race contacts per ball.

The objective of the work reported herein was to conduct a fatigue life analysis of the arched outer-race ball bearing and to compare the

fatigue life of this bearing with that of a conventional bearing at various combinations of thrust load and speed. A first order thrust load analysis, in which gyroscopic, elastohydrodynamic, and thermal effects are neglected, is reported. A more detailed report of the above is given by the authors in reference-12.

### SYMBOLS

- A distance between raceway groove curvature centers  
 / right side outer race curvature center  
 a semimajor axis of the projected contact ellipse  
 B  $f_0 + f_1 - 1 = A/D$   
 / ball center initially  
 b semiminor axis of the projected contact ellipse  
 / initial position, inner raceway groove curvature center  
 D ball diameter  
 / left side outer race curvature center  
 d raceway diameter  
 $d_m$  pitch diameter  
 E  $\frac{L|_{a=0.005} - L|_{a=0}}{L|_{a=0}} \cdot 100$  = percent improvement of an arch bearing  
 (a = 0.005) over that of a conventional bearing (a = 0)  
 / elliptical integral of the second kind  
 $F$  axially applied load  
 / centrifugal force  
 F  $r^2$   
 e amount of arching, or width of material removed from outer race of conventional bearing

- $h$  distance from top of arch to top of ball when the bearing is in a radial contact position  
 $K$  load deflection constant  
 $k$   $a/b$   
 $L$  life in hours  
 $Z$  ball center, finally  
 $Z'$  final position, inner raceway groove curvature center  
 $r_c$  tip of arch  
 $n$  rotational speed  
 $P$  basic dynamic capacity of a raceway contact  
 $P_d$  bearing diametral clearance  
 $P_e$  free endplay  
 $Q$  ball normal load  
 $r$  raceway groove curvature radius  
 $S$  distance between inner and outer raceway groove curvature center loci  
 $S_d$  diametral play  
 $T$   $\tau_o/\sigma_{max}$   
 $T_1$   $(\tau_o/\sigma_{max})_{k=1}$   
 $u$  number of stress cycles per revolution  
 $V$  radial projection of distance between ball center and outer raceway groove curvature center  
 $W$  axial projection of distance between ball center and outer raceway groove curvature center  
 $z$  number of balls  
 $\alpha$  radial contact angle

|                 |  |
|-----------------|--|
| $\beta$         | axial contact angle  |
| $\gamma$        | $D \cos \beta / \bar{d}_m$   |
| $\Delta$        | distance between raceway groove curvature center and final position of ball center |
| $\delta$        | contact deformation  |
| $\delta_a$      | axial displacement   |
| $\xi$           | ratio of depth of maximum shear stress to semi-minor axis, $\xi_0 = b$             |
| $\zeta_1$       | $(\zeta)_{k=1}$  |
| $\eta$          | defined by equation (8)  |
| $\rho$          | curvature sum  |
| $\sigma_{\max}$ | maximum normal stress  |
| $\tau_0$        | maximum orthogonal subsurface shear stress   |

## Subscripts:

|    |                               |
|----|-------------------------------|
| i  | refers to inner raceway       |
| o  | refers to outer raceway       |
| 01 | refers to left outer raceway  |
| 02 | refers to right outer raceway |
| x  | refers to x direction         |
| z  | refers to z direction         |

Barred values refer to final position

### ARCHED BEARING GEOMETRY

Figure 1 shows how the arched outer race is made. A conventional outer race is shown in figure 1(a) with race radius of  $r$ . Also shown in figure 1(a) is the portion of the conventional outer race that is removed in forming an arched outer race. Figure 1(b) shows the arched outer race with the portion of length  $2r$  removed. Note that there are now two outer

race radius centers separated by a distance  $g$ .

Figure 2 shows the arched bearing while in a noncontacting position. Here the pitch diameter ( $d_m$ ), and diametral clearance ( $P_d$ ), diametral play ( $S_d$ ), and raceway diameters ( $d_i, d_o$ ) are defined. The diametral play is the total amount of radial movement allowed in the bearing. Furthermore the diametral clearance is the diametral play plus two times the distance from the bottom of the ball to the tip of the arch when the bearing is in a radial contact position.

Figure 3 shows the arched bearing in a radial contact position. Instead of contacting at one point at the bottom of the outer raceway the ball contacts at two points separated by an angle  $2\alpha$ . From figure 3 the radial contact angle  $\alpha$  can be written as

$$\alpha = \sin^{-1} \left( \frac{g}{2r_o - D} \right) \quad (1)$$

A distance which needs to be formulated is the distance from the tip of the arch to the bottom of the ball when the ball and raceway are in the radial contact position as shown in figure 3. This distance will be defined as  $h$ . From figure 3(b) and using the Pythagorean theorem the following can be written

$$r_o^2 - \left( r_o - \frac{D}{2} \right)^2 \sin^2 \alpha + \left[ h + \frac{D}{2} + \left( r_o - \frac{D}{2} \right) \cos \alpha \right]^2$$

Solving for  $h$  the following can be written

$$h = -\frac{D}{2} - \left( r_o - \frac{D}{2} \right) \cos \alpha + \frac{1}{2} \left[ D(4r_o - D) + (2r_o - D)^2 \cos^2 \alpha \right]^{1/2} \quad (2)$$

Note that, as one might expect, as  $\alpha \rightarrow 0^\circ$   $h \rightarrow 0$ . Knowing  $h$ , from figures 2 and 3 a number of conventional bearing parameters can be formulated. The outer raceway diameter may be written as

$$d_o = d_i + P_d + 2D \quad (3)$$

where

$$P_d = S_d + 2h \quad (4)$$

From equations (3) and (4) the diametral play can be written as

$$S_d = d_o - d_i - 2D - 2h \quad (5)$$

The pitch diameter  $d_m$  from figure 2 can be expressed as

$$d_m = d_i + \frac{S_d}{2} + D \quad (6)$$

Figure 4 shows the arched ball bearing while in the axial contact position. Note, the ball is in the top position. From this figure the distance between the center of curvature of the inner and right outer race can be written as

$$A = r_o + r_i - D = BD \quad (7)$$

where

$$B = f_o + f_i - 1$$

$$f_o = \frac{r_o}{D}$$

and

$$f_i = \frac{r_i}{D}$$

From figure 4(b) the following equation can be written

$$r_o^2 = \left(\frac{g}{2}\right)^2 + (r_o - \eta)^2$$

Solving for  $\eta$  one gets

$$\eta = r_0 - \sqrt{r_0^2 - \left(\frac{g}{2}\right)^2} \quad (8)$$

Knowing  $\eta$ , the axial contact angle can be written as

$$\beta = \cos^{-1} \left( \frac{A - \frac{P_d}{2} - \eta}{A} \right) \quad (9)$$

The end play of an arched bearing is

$$P_e = 2A \sin \beta - g \quad (10)$$

## ANALYSIS

### Contact Geometry

From the experimental work of Haines and Edmonds (ref. 11) it is observed that the arched bearing will initially operate with two point contact at the lower speeds and then with three point contact at higher speeds when the centrifugal forces become significant. When centrifugal force acts on the ball, the inner and outer raceway contact angles are dissimilar, therefore, the lines of action between raceway groove curvature radius centers become discontinuous as shown in figure 5. In this figure the right and left outer raceway groove curvature centers ( $\mathcal{O}$  and  $\mathcal{O}'$ ) are fixed in space and the inner raceway groove curvature center ( $\mathcal{C}$ ) moves axially relative to these fixed centers.

Following the general approach used by reference 13 and using figure 5, the distance between the fixed right and left outer raceway groove curvature centers ( $\mathcal{O}$  and  $\mathcal{O}'$ ) and the final position of the ball center ( $\mathcal{L}$ ) can be written as

$$\Delta_{01} = r_o - \frac{D}{2} + \delta_{01} = (f_o - 0.5)D + \delta_{01} \quad (11)$$

$$\Delta_{02} = (f_o - 0.5)D + \delta_{02} \quad (12)$$

where  $\delta_{01}$  = normal contact deformation at left outer raceway center, and  $\delta_{02}$  = normal contact deformation at right outer raceway center. Similarly the distance between the final inner raceway groove curvature center ( $\mathcal{N}$ ) and the final position of the ball center ( $\mathcal{Z}$ ) is

$$\Delta_i = (f_i - 0.5)D + \delta_i \quad (13)$$

where  $\delta_i$  = normal contact deformation at the inner raceway center.

The axial distance between the final position of the inner and right outer raceway groove center is

$$S_x = A \sin \beta + \delta_a \quad (14)$$

where  $\delta_a$  = axial displacement. The radial distance between the final position of the inner raceway groove curvature center and the right or left outer raceway groove curvature center is

$$S_z = A \cos \beta \quad (15)$$

From figure 5 and equations (11) through (15) the following can be written

$$\cos \beta_{01} = \frac{V}{(f_o - 0.5)D + \delta_{01}} \quad (16)$$

$$\sin \beta_{01} = \frac{g - W}{(f_o - 0.5)D + \delta_{01}} \quad (17)$$

$$\cos \beta_{02} = \frac{V}{(f_o - 0.5)D + \delta_{02}} \quad (18)$$

$$\sin \beta_{02} = \frac{W}{(f_o - 0.5)D + \delta_{02}} \quad (19)$$

$$\cos \beta_i = \frac{A \cos \beta - V}{(f_i - 0.5)D + \delta_i} \quad (20)$$

$$\sin \beta_i = \frac{A \sin \beta + \delta_a - W}{(f_i - 0.5)D + \delta_i} \quad (21)$$

Using the Pythagorean theorem and regrouping terms the following can be written

$$\delta_{01} = -\sqrt{V^2 + (g - W)^2} - D(f_o - 0.5) \quad (22)$$

$$\delta_{02} = -\sqrt{V^2 + W^2} - D(f_o - 0.5) \quad (23)$$

$$\delta_i = -\sqrt{(A \cos \beta - V)^2 + (A \sin \beta + \delta_a - W)^2} - D(f_i - 0.5) \quad (24)$$

The normal loads shown in figure 6 are related to the normal contact deformation in the following way

$$Q = K\delta^{1.5} \quad (25)$$

With proper subscripting of  $i$ ,  $01$ , and  $02$  this equation could represent the normal loads of the inner ring ( $Q_i$ ) left outer ring ( $Q_{01}$ ), or right outer ring ( $Q_{02}$ ). From figure 6 the equilibrium of the forces in the horizontal and vertical directions are

$$Q_i \sin \beta_i + Q_{01} \sin \beta_{01} - Q_{02} \sin \beta_{02} = 0$$

$$Q_i \cos \beta_i - Q_{01} \cos \beta_{01} - Q_{02} \cos \beta_{02} + F_c = 0$$

Substituting equations (14) through (21) and equation (25) into the above equations gives the following

$$\frac{K_i \delta_i^{1.5} (S_x - W)}{(f_i - 0.5)D + \delta_i} - \frac{K_{02} \delta_{02}^{1.5} W}{(f_o - 0.5)D + \delta_{02}} + \frac{K_{01} \delta_{01}^{1.5} (g - W)}{(f_o - 0.5)D + \delta_{01}} = 0 \quad (26)$$

$$\frac{K_i \delta_i^{1.5} (S_z - V)}{(f_i - 0.5)D + \delta_i} - \frac{K_{02} \delta_{02}^{1.5} V}{(f_o - 0.5)D + \delta_{02}} - \frac{K_{01} \delta_{01}^{1.5} V}{(f_o - 0.5)D + \delta_{01}} + F_c = 0 \quad (27)$$

The expression for the load deflection constants ( $K_i$ ,  $K_{01}$ , and  $K_{02}$ ), the centrifugal force ( $F_c$ ), and the axial contact displacement ( $\delta_a$ ) are developed by the authors in reference 12 and will not be repeated here. Knowing these expressions ( $K_i$ ,  $K_{01}$ ,  $K_{02}$ ,  $F_c$ , and  $\delta_a$ ) one can solve for  $V$  and  $W$  in equations (26) and (27). The Newton-Raphson iteration method was used to solve the system of nonlinear equations. Knowing  $V$  and  $W$  and given equations (16) through (25) the contact loads ( $Q_i$ ,  $Q_{01}$ ,  $Q_{02}$ ) and angles ( $\beta_i$ ,  $\beta_{01}$ ,  $\beta_{02}$ ) can be evaluated.

#### Derivation of Fatigue Life

From the weakest link theory, on which the Weibull equation is based, we get the relationship between life of an assembly (the bearing) and its components (the inner and outer rings) as

$$\frac{1}{L} = \left( \frac{12n_i}{1 \times 10^6} \right) \left[ \left( \frac{1}{L_i} \right)^{10/9} + \left( \frac{1}{L_{01}} \right)^{10/9} + \left( \frac{1}{L_{02}} \right)^{10/9} \right]^{9/10} \quad (28)$$

In this equation life  $L$  is expressed in hours. A material improvement factor of five has been assumed, however no adjustment factors for reliability or operating conditions has been added. For point contact

$$L = \left( \frac{P}{Q} \right)^3 \quad (29)$$

Therefore equation (28) becomes

$$L = \left( \frac{1 \times 10^6}{12n_i} \right) \frac{1}{\left[ \left( \frac{Q_i}{P_i} \right)^{10/3} + \left( \frac{Q_{01}}{P_{01}} \right)^{10/3} + \left( \frac{Q_{02}}{P_{02}} \right)^{10/3} \right]^{0.9}} \quad (30)$$

The contact loads are defined by equation (25). From Lundberg and Palmgren (ref. 14) the following can be written

$$P = (84\ 000)D^{1.8} \left[ \frac{T_1}{T} \right]^{3.1} \left[ \frac{\xi}{\xi_1} \right]^{0.4} \left( \frac{2E}{\pi D \rho} \right)^{2.1} (k)^{0.7} \left[ \frac{D}{d} \right]^{0.3} u^{-1/3} \quad (31)$$

With proper subscripting of  $i$ ,  $01$ , and  $02$  this equation can represent the dynamic loads of the inner ring ( $P_i$ ), the left outer ring ( $P_{01}$ ), and the right outer ring ( $P_{02}$ ).

Variations of the  $T$  and  $\xi$  functions with curvature over the range from 0.52 to 0.54 are 2.3 and 0.8 percent, respectively. The variation of the product of these functions over the curvature range from 0.52 to 0.54 is less than 2 percent. Therefore, for the range described above the products of the  $T$  and  $\xi$  functions can be considered a constant in equation (31) or

$$\left[ \frac{T_1}{T} \right]^{3.1} \left[ \frac{\xi}{\xi_1} \right]^{0.4} = 0.718 \quad (32)$$

The number of stress cycles per revolution for each contact is, to a good approximation (ref. 14)

$$u_i = \frac{Z}{2} (1 + \gamma_i) \quad (33)$$

$$u_{01} = \frac{Z}{2} (1 - \gamma_{01}) \quad (34)$$

$$u_{02} = \frac{Z}{2} (1 - \gamma_{02}) \quad (35)$$

Substituting equations (32) through (35) into equation (31), one can obtain the dynamic capacity at inner ring, left and right outer rings as

$$P_i = \frac{60\,312}{(d_i)^{0.3}} \left( \frac{2\mathcal{E}_i}{\pi\rho_i} \right)^{2.1} (k_i)^{0.7} \left[ \frac{z}{2} (1 + \gamma_i) \right]^{-1/3} \quad (36)$$

$$P_{01} = \frac{60\,312}{(d_o)^{0.3}} \left( \frac{2\mathcal{E}_{01}}{\pi\rho_{01}} \right)^{2.1} (k_{01})^{0.7} \left[ \frac{z}{2} (1 - \gamma_{01}) \right]^{-1/3} \quad (37)$$

$$P_{02} = \frac{60\,312}{(d_o)^{0.3}} \left( \frac{2\mathcal{E}_{02}}{\pi\rho_{02}} \right)^{2.1} (k_{02})^{0.7} \left[ \frac{z}{2} (1 - \gamma_{02}) \right]^{-1/3} \quad (38)$$

Therefore from equations (25), (36) through (38), and equation (30), the life in hours of the bearing can be obtained. The equations for a conventional bearing can be directly obtained from the arched bearing analysis by simply letting the amount of arching be zero ( $g = 0$ ) and not considering equations related to the left outer race.

### DISCUSSION OF RESULTS

A conventional 150-mm ball thrust bearing was used for the computer evaluation. Bearing parameters and results such as life, contact loads and angles for various speeds and axial loads are shown in table I for the conventional bearing. Then calculations were made for the arched bearing (fig. 1(b)). The diametral play ( $S_d$ ) (fig. 2) was set fixed at 0.2499 mm (0.0098 in.) for all the results presented. In an arch bearing the free contact angle becomes larger than that of the conventional bearing even though the diametral play is held constant. The greater the amount of arching (the larger  $g$ ) the higher the free contact angle. Also some of the other bearing geometry parameters were changed by changing the amount of arching. Tables II and III show the effect of the amount of arching on life, contact loads, and angles while varying speeds and axial loads.

The following observations can be made from the results in Tables I through III:

1. For high speeds ( $n_1 = 20\,000$  rpm) there is a substantial increase in life for an arched bearing when compared to a conventional bearing.

2. At high speeds and light loads the longest life is obtained with a  $g$  of 0.127 mm (0.005 in.).

3. There is less advantage in an arched bearing at high loads ( $F_a \geq 13\,345$  N (3000 lb)).

4. For low speeds the arched bearing does not offer the advantages that it does for high speed applications.

5. At low speeds and small amounts of arching the arch bearing operates at a two point contact.

6. As the applied load ( $F_a$ ) increases the initial speed for three point contact increases.

7. As the amount of arching is increased, the speed where the arched bearing has initial three point contact decreases.

8. Even small contact loads ( $Q_{01} \approx 100$  N (22.48 lb)) at the left outer race help to improve the life significantly over a conventional bearing.

Figure 7 shows the percent improvement in fatigue life of an arched bearing ( $g = 0.127$  mm (0.005 in.)) over that of a conventional bearing for axial loads of 4448 N (1000 lb), 13 345 N (3000 lb), and 22 241 N (5000 lb). The ordinate  $E$  of this figure is defined by the following relationship

$$E = \left[ \frac{L|_{g=0.005} - L|_{g=0}}{L|_{g=0}} \right] 100 \quad (39)$$

In this figure we see that there is significant improvement over the conventional bearing for high speed applications. For example, at  $n_i = 28\,000$  rpm and  $F_a = 4448$  N (1000 lb), the improvement in life of an arched bearing ( $g = 0.127$  mm (0.005 in.)) is 340 percent. As the applied load ( $F_a$ ) increases the advantage of the arched bearing becomes less significant.

#### SUMMARY OF RESULTS

A first order thrust load analysis of an arched bearing which considers centrifugal forces but which neglects gyroscopics, elastohydrodynamics, and thermal effects was performed. A Newton-Raphson method of iteration was used in evaluating the radial and axial projection of the distance between the ball center and the outer raceway groove curvature center ( $V$  and  $W$ ).

Fatigue life evaluations were made. The similar analysis of a conventional bearing can be directly obtained from the arched bearing analysis by simply letting the amount of arching be zero ( $g = 0$ ) and not considering equations related to the unloaded half of the outer race.

Computer solutions were obtained for a 150-mm bore ball bearing. The amount of arching investigated was from zero to a value of  $g = 0.762$  mm (0.030 in.). Results are as follows:

1. The arched bearing shows significant improvements in fatigue life over a conventional bearing, especially at high speeds. In particular at an axial load of 4448 N (1000 lb) the life improvement is 306 percent at 3 million DN and 340 percent at 4.2 million DN.

2. There is an optimal value of  $g$ , the amount of arching, to produce maximum life for a given diametral play and a given speed and load condition. For the particular bearing investigated life improvement was greatest at a 4448 N (1000 lb) thrust load and 28 000 rpm when  $g$  was 0.127 mm (0.005 in.).

3. For low speeds the arched bearing does not offer the advantages that it does for high speed applications.

#### REFERENCES

1. Brown, P. F., "Bearings and Dampers for Advanced Jet Engines," Paper 700318, Apr. 1970, SAE, New York, N. Y.
2. Jones, A. B., "Ball Motion and Sliding Friction in Ball Bearings," Journal of Basic Engineering, Vol. 81, No. 1, Mar. 1959, pp. 1-12.
3. Harris, T. A., "An Analytical Method to Predict Skidding in Thrust-Loaded, Angular-Contact Ball Bearings," Journal of Lubrication Technology, Vol. 93, No. 1, Jan. 1971, pp. 17-24.
4. Coe, H. H., Parker, R. J., and Scibbe, H. W., "Evaluation of Electron-Beam Welded Hollow Balls for High-Speed Ball Bearings," Journal of Lubrication Technology, Vol. 93, No. 1, Jan. 1971, pp. 47-59.

5. Coe, H. H., Scibbe, H. W., and Anderson, W. J., "Evaluation of Cylindrically Hollow (Drilled) Balls in Ball Bearings at DN Values to 2.1 Million," TN D-7007, 1971, NASA, Cleveland, Ohio.
6. Holmes, P., "Evaluation of Drilled Ball Bearings at DN Values to 3 Million. Part I - Variable Oil Flow Tests," Proposed NASA Contractor Report.
7. Holmes, P., "Evaluation of Drilled Ball Bearings at DN Values to 3 Million. Part II - Experimental Skid Study and Endurance Tests," Proposed NASA Contractor Report.
8. Wilcock, D. F., and Winn, L. W., "The Hybrid Boost Bearing - A Method of Obtaining Long Life in Rolling Contact Bearing Applications," Journal of Lubrication Technology, Vol. 92, No. 3, July 1970, pp. 406-414.
9. Anderson, W. J., Fleming, D. P., and Parker, R. J., "The Series Hybrid Bearing - A New High Speed Bearing Concept," Paper 71-LUB-15, 1971, ASME, New York, N. Y.
10. Nypan, L. J., Hamrock, B. J., Scibbe, H. W., and Anderson, W. J., "Optimization of Conical Hydrostatic Bearing for Minimum Friction," Paper 71-LUB-19, 1971, ASME, New York, N. Y.
11. Hanes, D. J., and Edmonds, M. J., "A New Design of Angular Contact Ball Bearing," Proceedings of the Institution of Mechanical Engineers, Vol. 185, 1970/1971, pp. 382-393.
12. Hamrock, B. J., and Anderson, N. J., "Analysis of an Arched Outer-Race Ball Bearing Considering Centrifugal Forces," Proposed NASA TN.
13. Harris, T. A., Rolling Bearing Analysis, Wiley, New York, 1966.
14. Lundberg, G., and Palmgren, A., "Dynamic Capacity of Rolling Bearings," Acta Polytechnica, Mechanical Engineering Series, Vol. 1, No. 3, Issue 7, 1947.

TABLE I. - CONVENTIONAL BEARING (50 LIFE, CONTACT LOADS AND ANGLES FOR VARIOUS SPEEDS AND AXIAL APPLIED FORCES

[Bearing data:  $r_1 = 0.54$ ,  $r_2 = 0.52$ ,  $d_m = 187.55$  mm (7.3838 in.),  $D = 22.23$  mm (0.8750 in.),  $\delta_d = 0.2499$  mm (0.0098 in.),  $\alpha = 25^\circ$ ,  $z = 22$ ]

| F, N<br>N lbs    | $n_1$ , rpm |           |            |           |            |         |            |         |            |         |            |        |            |          |
|------------------|-------------|-----------|------------|-----------|------------|---------|------------|---------|------------|---------|------------|--------|------------|----------|
|                  | 4060        | 8000      | 12 000     | 16 000    | 20 000     | 24 000  | 28 000     |         |            |         |            |        |            |          |
| 4438<br>(10000)  | L           | 84 727 hr | L          | 11 478 hr | L          | 450 hr  | L          | 130 hr  | L          | 45 hr   |            |        |            |          |
|                  | $Q_1$       | 326.3 N   | $Q_1$      | 376.0 N   | $Q_1$      | 368.1 N | $Q_1$      | 354.5 N | $Q_1$      | 347.9 N |            |        |            |          |
|                  | $Q_{02}$    | 570.1 N   | $Q_{02}$   | 1911 N    | $Q_{02}$   | 3167 N  | $Q_{02}$   | 4809 N  | $Q_{02}$   | 6849 N  |            |        |            |          |
|                  | $\alpha$    | 29.31°    | $\alpha$   | 32.53°    | $\alpha$   | 33.22°  | $\alpha$   | 34.04°  | $\alpha$   | 34.77°  |            |        |            |          |
|                  | $\alpha_2$  | 20.77°    | $\alpha_2$ | 11.25°    | $\alpha_2$ | 6.075°  | $\alpha_2$ | 2.411°  | $\alpha_2$ | 1.693°  |            |        |            |          |
| 1345<br>(3000)   | L           | 19 432 hr | L          | 6996 hr   | L          | 3163 hr | L          | 1007 hr | L          | 302 hr  | L          | 99 hr  | L          | 37 hr    |
|                  | $Q_1$       | 1297 N    | $Q_1$      | 1208 N    | $Q_1$      | 1138 N  | $Q_1$      | 1098 N  | $Q_1$      | 1072 N  | $Q_1$      | 1050 N | $Q_1$      | 1030 N   |
|                  | $Q_{02}$    | 1433 N    | $Q_{02}$   | 1799 N    | $Q_{02}$   | 2579 N  | $Q_{02}$   | 3796 N  | $Q_{02}$   | 5427 N  | $Q_{02}$   | 7466 N | $Q_{02}$   | 9924 N   |
|                  | $\alpha$    | 27.88°    | $\alpha$   | 30.14°    | $\alpha$   | 32.20°  | $\alpha$   | 33.53°  | $\alpha$   | 34.48°  | $\alpha$   | 35.29° | $\alpha$   | 36.08°   |
|                  | $\alpha_2$  | 23.03°    | $\alpha_2$ | 19.70°    | $\alpha_2$ | 13.60°  | $\alpha_2$ | 9.192°  | $\alpha_2$ | 6.417°  | $\alpha_2$ | 4.659° | $\alpha_2$ | 3.503°   |
| 22 241<br>(5000) | L           | 3060 hr   | L          | 1640 hr   | L          | 1016 hr | L          | 500 hr  | L          | 199 hr  | L          | 76 hr  | L          | 30 hr    |
|                  | $Q_1$       | 2137 N    | $Q_1$      | 2030 N    | $Q_1$      | 1915 N  | $Q_1$      | 1833 N  | $Q_1$      | 1778 N  | $Q_1$      | 1737 N | $Q_1$      | 1702 N   |
|                  | $Q_{02}$    | 2271 N    | $Q_{02}$   | 2598 N    | $Q_{02}$   | 3293 N  | $Q_{02}$   | 4440 N  | $Q_{02}$   | 6035 N  | $Q_{02}$   | 8060 N | $Q_{02}$   | 10 515 N |
|                  | $\alpha$    | 28.23°    | $\alpha$   | 29.87°    | $\alpha$   | 31.86°  | $\alpha$   | 33.47°  | $\alpha$   | 34.65°  | $\alpha$   | 35.60° | $\alpha$   | 36.44°   |
|                  | $\alpha_2$  | 26.43°    | $\alpha_2$ | 22.90°    | $\alpha_2$ | 17.88°  | $\alpha_2$ | 13.16°  | $\alpha_2$ | 9.642°  | $\alpha_2$ | 7.204° | $\alpha_2$ | 5.516°   |

TABLE II ARCH WEARING LIFE, CONTACT LOADS, AND ANGLES FOR VARIOUS SPEEDS AND AXIAL

APPLIED FORCES

[Beam: dia: 1.054,  $f_0$  0.52,  $d_{in}$  157.55 mm (7.3838 in.), D 22.23 mm (0.8750 in.),  
 $S_d$  0.2499 mm (0.0098 in.),  $\alpha$  25.46°, z 22, g 0.127 mm (0.005 in.)]

| F <sub>ax</sub><br>N/hr | n <sub>1</sub> , rpm    |                         |                         |                         |                        |                        |                        |  |  |  |  |  |
|-------------------------|-------------------------|-------------------------|-------------------------|-------------------------|------------------------|------------------------|------------------------|--|--|--|--|--|
|                         | 7000                    | 8000                    | 12000                   | 16000                   | 20000                  | 24000                  | 28000                  |  |  |  |  |  |
| 4435<br>(10000)         | L 358.806 hr            | L 89.881 hr             | L 26.290 hr             | L 6804 hr               | L 1625 hr              | L 560 hr               | L 198 hr               |  |  |  |  |  |
|                         | Q <sub>1</sub> 419.5 N  | Q <sub>1</sub> 384.2 N  | Q <sub>1</sub> 379.3 N  | Q <sub>1</sub> 375.0 N  | Q <sub>1</sub> 370.5 N | Q <sub>1</sub> 366.0 N | Q <sub>1</sub> 361.4 N |  |  |  |  |  |
|                         | Q <sub>01</sub> 0 N     | Q <sub>01</sub> 20.01 N | Q <sub>01</sub> 503.4 N | Q <sub>01</sub> 1178 N  | Q <sub>01</sub> 2031 N | Q <sub>01</sub> 3068 N | Q <sub>01</sub> 4292 N |  |  |  |  |  |
|                         | Q <sub>02</sub> 563.4 N | Q <sub>02</sub> 1015 N  | Q <sub>02</sub> 1404 N  | Q <sub>02</sub> 1963 N  | Q <sub>02</sub> 2727 N | Q <sub>02</sub> 3682 N | Q <sub>02</sub> 4837 N |  |  |  |  |  |
|                         | $\beta_1$ 31.41°        | $\beta_1$ 31.76°        | $\beta_1$ 32.21°        | $\beta_1$ 32.63°        | $\beta_1$ 33.07°       | $\beta_1$ 33.53°       | $\beta_1$ 34.01°       |  |  |  |  |  |
|                         | $\beta_{01}$ 0°         | $\beta_{01}$ 4.645°     | $\beta_{01}$ 5.761°     | $\beta_{01}$ 6.316°     | $\beta_{01}$ 6.655°    | $\beta_{01}$ 6.867°    | $\beta_{01}$ 6.996°    |  |  |  |  |  |
|                         | $\beta_{02}$ 10.62°     | $\beta_{02}$ 11.59°     | $\beta_{02}$ 10.37°     | $\beta_{02}$ 9.698°     | $\beta_{02}$ 9.236°    | $\beta_{02}$ 8.892°    | $\beta_{02}$ 8.621°    |  |  |  |  |  |
| 13347<br>(30000)        | L 14.036 hr             | L 7288 hr               | L 3411 hr               | L 1752 hr               | L 817 hr               | L 348 hr               | L 146 hr               |  |  |  |  |  |
|                         | Q <sub>1</sub> 1279 N   | Q <sub>1</sub> 1190 N   | Q <sub>1</sub> 1127 N   | Q <sub>1</sub> 1110 N   | Q <sub>1</sub> 1095 N  | Q <sub>1</sub> 1082 N  | Q <sub>1</sub> 1069 N  |  |  |  |  |  |
|                         | Q <sub>01</sub> 0 N     | Q <sub>01</sub> 0 N     | Q <sub>01</sub> 80.51 N | Q <sub>01</sub> 784.4 N | Q <sub>01</sub> 1701 N | Q <sub>01</sub> 2802 N | Q <sub>01</sub> 4087 N |  |  |  |  |  |
|                         | Q <sub>02</sub> 1415 N  | Q <sub>02</sub> 1783 N  | Q <sub>02</sub> 2492 N  | Q <sub>02</sub> 3006 N  | Q <sub>02</sub> 3691 N | Q <sub>02</sub> 4578 N | Q <sub>02</sub> 5675 N |  |  |  |  |  |
|                         | $\beta_1$ 26.31°        | $\beta_1$ 30.63°        | $\beta_1$ 32.57°        | $\beta_1$ 33.14°        | $\beta_1$ 33.63°       | $\beta_1$ 34.10°       | $\beta_1$ 34.58°       |  |  |  |  |  |
|                         | $\beta_{01}$ 0°         | $\beta_{01}$ 0°         | $\beta_{01}$ 1.879°     | $\beta_{01}$ 3.393°     | $\beta_{01}$ 4.339°    | $\beta_{01}$ 4.998°    | $\beta_{01}$ 5.467°    |  |  |  |  |  |
|                         | $\beta_{02}$ 25.38°     | $\beta_{02}$ 19.89°     | $\beta_{02}$ 14.15°     | $\beta_{02}$ 12.54°     | $\beta_{02}$ 11.49°    | $\beta_{02}$ 10.71°    | $\beta_{02}$ 10.11°    |  |  |  |  |  |
| 23241<br>(6000)         | L 3186 hr               | L 1717 hr               | L 1051 hr               | L 622 hr                | L 372 hr               | L 204 hr               | L 103 hr               |  |  |  |  |  |
|                         | Q <sub>1</sub> 2109 N   | Q <sub>1</sub> 2003 N   | Q <sub>1</sub> 1890 N   | Q <sub>1</sub> 1836 N   | Q <sub>1</sub> 1809 N  | Q <sub>1</sub> 1785 N  | Q <sub>1</sub> 1763 N  |  |  |  |  |  |
|                         | Q <sub>01</sub> 0 N     | Q <sub>01</sub> 0 N     | Q <sub>01</sub> 0 N     | Q <sub>01</sub> 48.37 N | Q <sub>01</sub> 1423 N | Q <sub>01</sub> 2567 N | Q <sub>01</sub> 3898 N |  |  |  |  |  |
|                         | Q <sub>02</sub> 2243 N  | Q <sub>02</sub> 2571 N  | Q <sub>02</sub> 3272 N  | Q <sub>02</sub> 3955 N  | Q <sub>02</sub> 4595 N | Q <sub>02</sub> 5428 N | Q <sub>02</sub> 6474 N |  |  |  |  |  |
|                         | $\beta_1$ 24.64°        | $\beta_1$ 30.32°        | $\beta_1$ 32.34°        | $\beta_1$ 33.41°        | $\beta_1$ 33.98°       | $\beta_1$ 34.49°       | $\beta_1$ 34.99°       |  |  |  |  |  |
|                         | $\beta_{01}$ 0°         | $\beta_{01}$ 0°         | $\beta_{01}$ 0°         | $\beta_{01}$ 0.9138°    | $\beta_{01}$ 2.310°    | $\beta_{01}$ 3.315°    | $\beta_{01}$ 4.060°    |  |  |  |  |  |
|                         | $\beta_{02}$ 26.79°     | $\beta_{02}$ 23.15°     | $\beta_{02}$ 18.00°     | $\beta_{02}$ 14.93°     | $\beta_{02}$ 13.44°    | $\beta_{02}$ 12.33°    | $\beta_{02}$ 11.46°    |  |  |  |  |  |

TABLE III - ARO of PLAINING LIFE, CONTACT LOADS AND ANGLES FOR VARIOUS SPEEDS AND AXIAL

APPLIED FORCES

Blanking die:  $d_1 = 0.54$ ,  $l_1 = 0.52$ ,  $d_m = 187.55$  mm (7.3838 in.),  $D = 22.23$  mm (0.8750 in.),  $d_2 = 0.259$  mm (0.010196 in.),  $r = 26.82$ ,  $\gamma = 22$ ,  $\mu = 0.254$  mm (0.010 in.)

| N hr         | $n_1$ , rpm  |              |              |              |              |              |              |              |              |              |              |              |              |        |
|--------------|--------------|--------------|--------------|--------------|--------------|--------------|--------------|--------------|--------------|--------------|--------------|--------------|--------------|--------|
|              | 4500         | 6000         | 12000        | 16000        | 20000        | 24000        | 28000        |              |              |              |              |              |              |        |
| 15000        | L            | 126 403 hr   | L            | 31 701 hr    | L            | 7 984 hr     | L            | 1 803 hr     | L            | 545 hr       | L            | 192 hr       |              |        |
|              | $Q_1$        | 400.5 N      | $Q_1$        | 378.4 N      | $Q_1$        | 354.2 N      | $Q_1$        | 369.8 N      | $Q_1$        | 365.2 N      | $Q_1$        | 360.6 N      |              |        |
|              | $Q_{01}$     | 0 N          | $Q_{01}$     | 644.8 N      | $Q_{01}$     | 1279 N       | $Q_{01}$     | 2101 N       | $Q_{01}$     | 3113 N       | $Q_{01}$     | 4320 N       |              |        |
|              | $Q_{02}$     | 545.1 N      | $Q_{02}$     | 847.7 N      | $Q_{02}$     | 1886 N       | $Q_{02}$     | 2681 N       | $Q_{02}$     | 3667 N       | $Q_{02}$     | 4848 N       |              |        |
|              | $\beta_1$    | 31.46°       | $\beta_1$    | 32.30°       | $\beta_1$    | 32.70°       | $\beta_1$    | 33.14°       | $\beta_1$    | 33.61°       | $\beta_1$    | 34.11°       |              |        |
|              | $\beta_{01}$ | 0°           | $\beta_{01}$ | 15.40°       | $\beta_{01}$ | 15.55°       | $\beta_{01}$ | 15.53°       | $\beta_{01}$ | 15.47°       | $\beta_{01}$ | 15.38°       |              |        |
|              | $\beta_{02}$ | 17.71°       | $\beta_{02}$ | 17.41°       | $\beta_{02}$ | 17.07°       | $\beta_{02}$ | 16.81°       | $\beta_{02}$ | 16.57°       | $\beta_{02}$ | 16.36°       |              |        |
|              | L            | 15 944 hr    | L            | 8 191 hr     | L            | 4 210 hr     | L            | 2 611 hr     | L            | 855 hr       | L            | 345 hr       | L            | 142 hr |
|              | $Q_1$        | 1228 N       | $Q_1$        | 1141 N       | $Q_1$        | 1115 N       | $Q_1$        | 1190 N       | $Q_1$        | 1091 N       | $Q_1$        | 1078 N       | $Q_1$        | 1065 N |
|              | $Q_{01}$     | 0 N          | $Q_{01}$     | 0 N          | $Q_{01}$     | 371.4 N      | $Q_{01}$     | 1020 N       | $Q_{01}$     | 1861 N       | $Q_{01}$     | 2896 N       | $Q_{01}$     | 4128 N |
| $Q_{02}$     | 1363 N       | $Q_{02}$     | 1736 N       | $Q_{02}$     | 2212 N       | $Q_{02}$     | 2800 N       | $Q_{02}$     | 3571 N       | $Q_{02}$     | 4533 N       | $Q_{02}$     | 5691 N       |        |
| $\beta_1$    | 29.60°       | $\beta_1$    | 32.10°       | $\beta_1$    | 32.96°       | $\beta_1$    | 33.36°       | $\beta_1$    | 33.78°       | $\beta_1$    | 34.23°       | $\beta_1$    | 34.71°       |        |
| $\beta_{01}$ | 0°           | $\beta_{01}$ | 0°           | $\beta_{01}$ | 14.12°       | $\beta_{01}$ | 14.38°       | $\beta_{01}$ | 14.52°       | $\beta_{01}$ | 14.60°       | $\beta_{01}$ | 14.62°       |        |
| $\beta_{02}$ | 26.42°       | $\beta_{02}$ | 26.42°       | $\beta_{02}$ | 18.37°       | $\beta_{02}$ | 17.88°       | $\beta_{02}$ | 17.49°       | $\beta_{02}$ | 17.14°       | $\beta_{02}$ | 16.84°       |        |
| 15000        | L            | 3591 hr      | L            | 1931 hr      | L            | 1180 hr      | L            | 707 hr       | L            | 396 hr       | L            | 204 hr       | L            | 100 hr |
|              | $Q_1$        | 2031 N       | $Q_1$        | 1926 N       | $Q_1$        | 1837 N       | $Q_1$        | 1816 N       | $Q_1$        | 1796 N       | $Q_1$        | 1776 N       | $Q_1$        | 1755 N |
|              | $Q_{01}$     | 0 N          | $Q_{01}$     | 0 N          | $Q_{01}$     | 132.2 N      | $Q_{01}$     | 778.2 N      | $Q_{01}$     | 1631 N       | $Q_{01}$     | 2682 N       | $Q_{01}$     | 3934 N |
|              | $Q_{02}$     | 2164 N       | $Q_{02}$     | 2496 N       | $Q_{02}$     | 3106 N       | $Q_{02}$     | 3683 N       | $Q_{02}$     | 4434 N       | $Q_{02}$     | 5373 N       | $Q_{02}$     | 6509 N |
|              | $\beta_1$    | 29.86°       | $\beta_1$    | 31.67°       | $\beta_1$    | 33.40°       | $\beta_1$    | 33.84°       | $\beta_1$    | 34.26°       | $\beta_1$    | 34.70°       | $\beta_1$    | 35.17° |
|              | $\beta_{01}$ | 0°           | $\beta_{01}$ | 0°           | $\beta_{01}$ | 12.84°       | $\beta_{01}$ | 13.31°       | $\beta_{01}$ | 13.60°       | $\beta_{01}$ | 13.78°       | $\beta_{01}$ | 13.90° |
|              | $\beta_{02}$ | 27.65°       | $\beta_{02}$ | 23.89°       | $\beta_{02}$ | 19.56°       | $\beta_{02}$ | 18.85°       | $\beta_{02}$ | 18.33°       | $\beta_{02}$ | 17.88°       | $\beta_{02}$ | 17.49° |

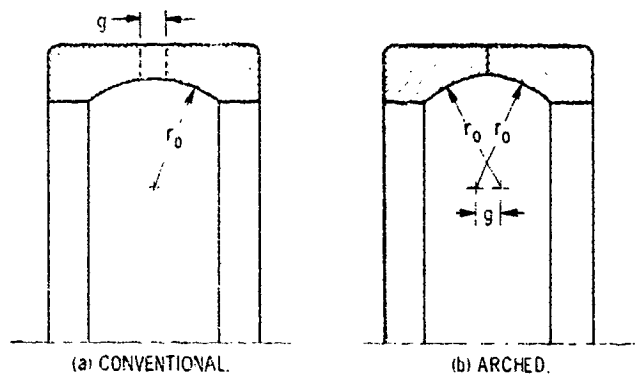


Figure 1 - Bearing outer race geometries.

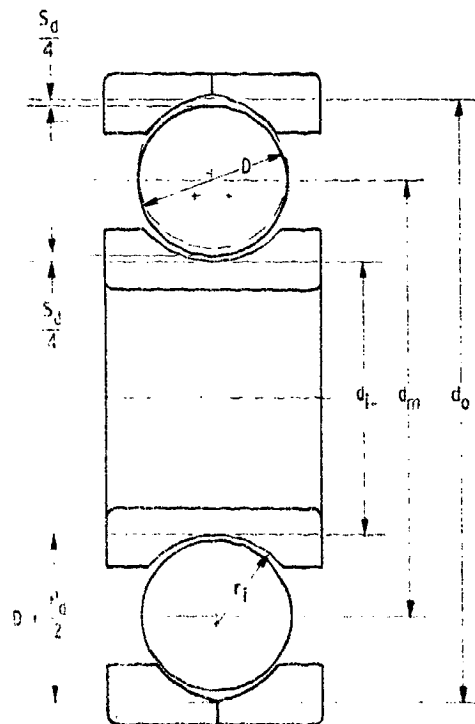
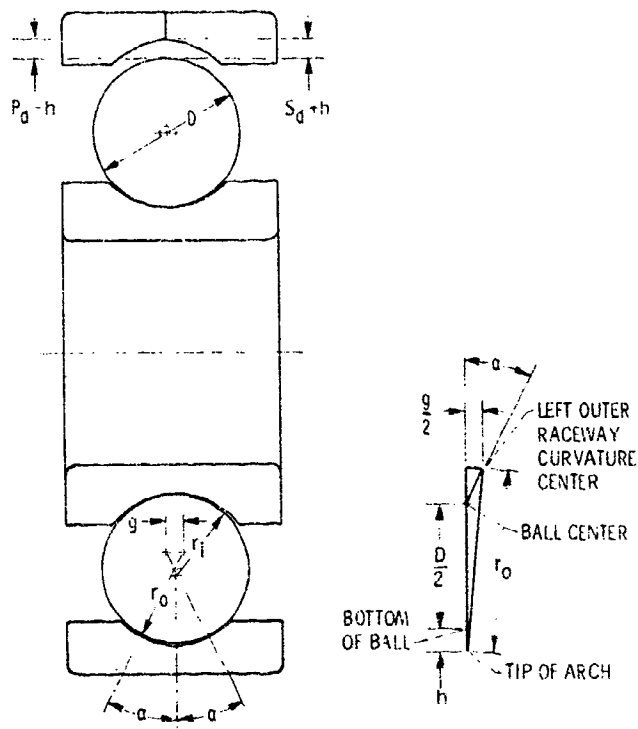


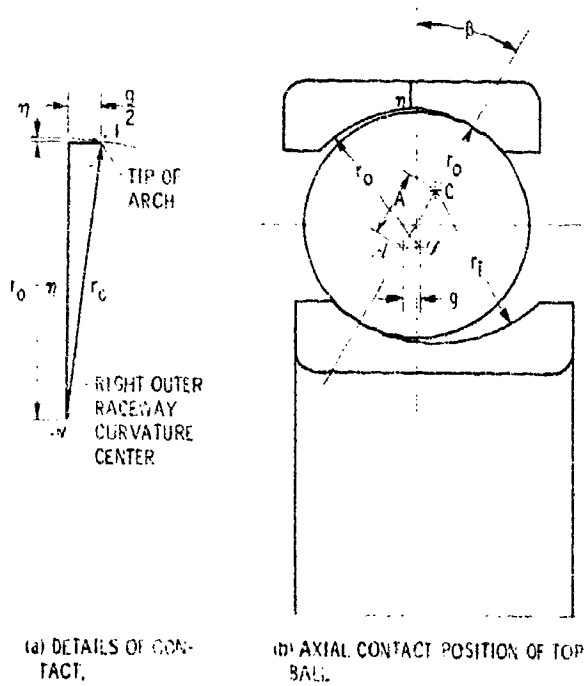
Figure 2 - Arched ball bearing in noncontacting position

E-6717



(a) RADIAL CONTACT POSITION. (b) DETAILS OF CONTACT.

Figure 3. - Arched ball bearing radially loaded.



(a) DETAILS OF CONTACT. (b) AXIAL CONTACT POSITION OF TOP BALL.

Figure 4. - Arched ball bearing axially loaded

- .A RIGHT SIDE OUTER RACE CURVATURE CENTER
- .B BALL CENTER, INITIALLY
- .C INNER RACEWAY GROOVE CURVATURE CENTER INITIALLY
- .D LEFT SIDE OUTER RACE CURVATURE CENTER
- .E BALL CENTER, FINALLY
- .H INNER RACEWAY GROOVE CURVATURE CENTER, FINALLY

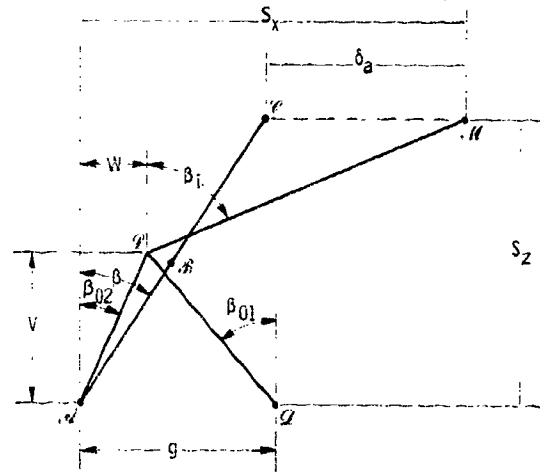


Figure 5. - Position of ball center and raceway groove curvature centers with and without centrifugal force acting on the ball. Points shown for ball in top position, with bearing loaded axially.

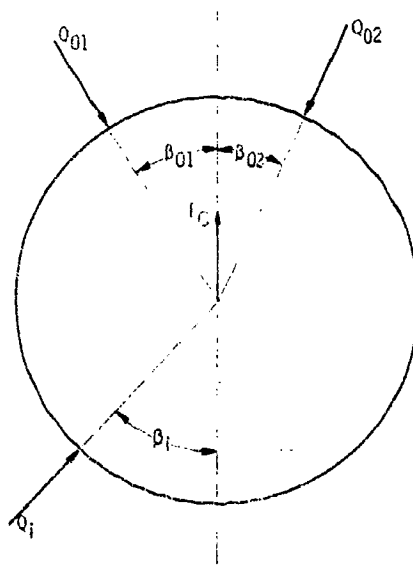


Figure 6. - Normal ball loading.

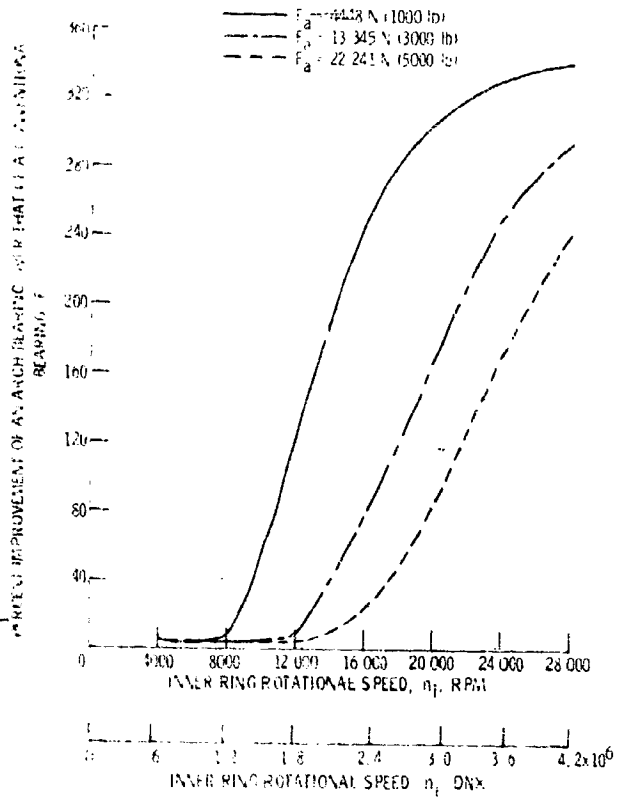


Figure 7. - Effect of speed on percent improvement of an arch bearing ( $\epsilon = 0.127$  mm or 0.005 in.) to that of a conventional bearing ( $\epsilon = 0$ ) for various axial applied loads.

**END  
DATE  
FILMED**

MAR 29 1972